High-power impulse magnetron sputtering and its applications*

Arutiun P. Ehiasarian

Nanotechnology Centre for PVD Research, Materials and Engineering Research Institute, Sheffield Hallam University, Howard St., Sheffield, S1 1WB, UK

Abstract: High-power impulse magnetron sputtering (HIPIMS) was introduced in the late 1990s as a unique physical vapor deposition method. The technology utilizes magnetron sputtering cathodes and high peak power density of up to 3 kW cm^{-2} on the target. The plasma produces a metal flux with high degree of ionization. HIPIMS has been successfully used as a substrate pretreatment method to enhance coating adhesion by promoting local epitaxial growth. As a deposition technology, HIPIMS produces high-density microstructure films. It has been industrialized and has successful applications in hard, electronic, and optical coatings.

Keywords: coating adhesion; high-density microstructure films; high-power impulse magnetron sputtering; local epitaxial growth; physical vapor deposition.

INTRODUCTION

Plasma-based thin film deposition processes have traditionally evolved toward higher ionization of the deposition flux to enhance film quality and enable high-precision processing on the nanoscale. The latest addition to this portfolio is the high-power impulse magnetron sputtering (HIPIMS) technology. The HIPIMS discharge is a type of high-current plasma glow which is typically characterized with a high burning voltage of 400–2000 V and a high-current density of 0.1–10 A cm^{-2}. HIPIMS discharges are homogeneously distributed over the cathode area and are distinctly different from arc discharges, which are constrained to individual cathode spots and have current density of $>10^3$ A cm^{-2}. The operation pressure is lower than diode sputtering, which necessitates a magnetic field to enhance ionization probability. HIPIMS is a type of high-current glow discharge, which today is upscaled to industry-standard magnetron sputtering cathodes.

High-current glow discharges have been in use since the 1960s when they were employed as spacecraft thrusters, plasma injectors for particle accelerators, lasers, and switchgear. Initially, the discharge was discovered as an intermediate stage of the gas breakdown process [1]. The stage has a few hundred volts and high-current density of several A cm^{-2} that could only be sustained over a limited period of time before converting to an arc with current density of 10^4 A cm^{-2}. These quasi-stationary or impulse discharges have been observed to conduct currents of 24 kA at 2000 V for 50 μs inside a 60-mm-diameter quartz tube. The usage of a low-density pre-ionizing discharge prior to the application of high power [1] to improve discharge stability was widespread.

The gas transits from low ionization directly to the quasi-stationary state and after a time period t_d may transit to the higher current density arc stage. The reverse transition from arc back to the quasi-stationary or glow discharge state is not possible. The duration, t_d, is determined by the pressure, overvoltage, and current but also by the thermal conductivity and resistivity of the cathode material.

Some of the first reports on the ionization degree in the deposition flux of the discharge are from Tyuryukanov et al. [2] and Kouznetsov et al. [3]. Ehiasarian et al. [4] showed that significant fractions of the Ar and metal atoms were ionized and that double-charged metal ions were present. Böhlmark et al. [5] used plasma sampling mass spectroscopy to show that the metal-to-Ar ion ratio is close to 1.

HIPIMS operates at significantly lower pressure of <10 mTorr, which is desired to allow efficient deposition rates. With magnetic fields of 30 mT, HIPIMS operates at a voltage of 1500 V, and current density of 2 A cm^{-2}. This is applied in impulses (short pulses) with low duty cycle of ~1 % and frequency ~200 Hz so that the average power of the discharge remains within standard cathode cooling.

Figure 1 shows a typical voltage and current waveform of an HIPIMS impulse operated on a 600 × 200 mm Nb cathode using an HMP4/2 power supply (Hüttinger Electronic Sp. z o.o.). The peak voltage is 2000 V, and the peak current is 3.5 kA. The voltage is switched off at the end of the pulse, and the current decays to 0 A within the next 50 µs. A very high peak plasma density of 10^{13} cm^{-3} [3,6] rich in metal ions is established near the substrates [4].
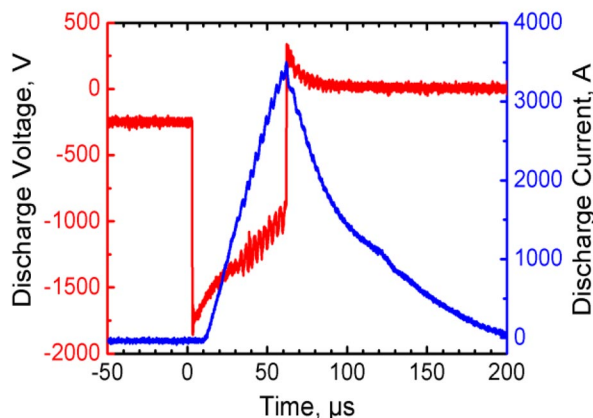
Fig. 1 Voltage and current waveforms during HIPIMS of Nb operation in Ar atmosphere at frequency of 100 Hz. The inset shows a photograph of the discharge and fast camera shots with 2 µs exposure.

The HIPIMS discharge is sustained by secondary electron emission by similar mechanisms as a conventional magnetron discharge. It is distributed homogeneously over the surface of the cathode throughout the duration of the pulse as shown in the inset of Fig. 1.

The discharge undergoes two stages in its temporal development. The initial stage is the ignition of Ar plasma followed by a metal ion dominated plasma [4]. Ar is strongly rarefied due to collisions with the sputtered metal.

HIPIMS is a stable discharge and has been demonstrated to work with a variety of elements such as B, C, Al, Si, Sc, Ti, V, Cr, Cu, Zn, Y, Zr, Nb, Mo, Ag, Ta, W, Au, as well as alloys such as TiAl, CrAl, TiAlY, and CrAlY in Ar, N_2, and O_2 atmospheres.

The current-voltage (*I–U*) characteristics of a discharge are a fingerprint that defines it. Conventional magnetron *I–U* characteristics follow a power law $I \sim kU^n$ where n is typically in the range 5–15 reaching low values when the discharge is confined by a weak magnetic field. Figure 2 shows the *I–U* characteristics of DC and HIPIMS magnetron discharges operated on an industrial size rectangular cathode and ø50 mm cathode [4] operated at a pressure of 0.4 Pa (3 mTorr). The exponent
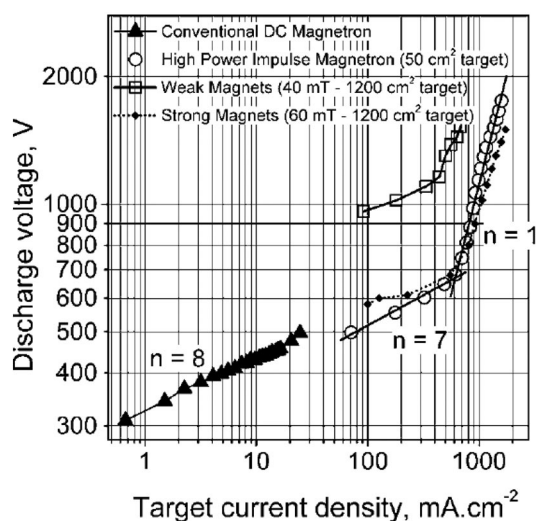
Fig. 2 *I–U* characteristics of the pulsed discharge. The exponent *n* of the power law $I \sim kU^n$ is indicated. Cr sputtering in Ar atmosphere at a pressure of 0.4 Pa (3 mTorr).

for the conventional magnetron is 8. The exponent for the pulsed discharge changes from 7 to 1 as the target current exceeds ~600 mA cm^{-2}. This change may be because secondary electrons accelerated in the sheath to 1.6 keV cannot be trapped by the magnetic field and the probability of ionizing collisions per electron is decreased. Furthermore, the generation of more metal-rich plasma reduces the potential secondary electron emission coefficient.

At the higher powers, the plasma density at the position of the substrate increases faster than at low powers [4] possibly due to the escape of plasma from the target confinement, extension of the ionization volume due to the greater voltage and cathode sheath, and the onset of self-sputtering.

In the HIPIMS discharge, although the sputtering voltage can be at least two times higher than DC, the sputtered atoms leave the target with the same energy of a few eV. However, they cannot penetrate the dense hot electron cloud formed at high discharge power without collisions, and the probability of ionization of the pulse-sputtered flux is high [4]. A portion of metal ions is accelerated back to the target surface [4], and although this gives rise to self-sputtering whose yield is similar to gas sputtering, the primary metal ion is absorbed by the target and cannot contribute to deposition [7]. The deposition flux at a distance of 50 cm from a Cr target surface was found to contain 30 % metal ions for peak target power of 1.5 kW cm^{-2} [4].

Typically, one- and two-fold ionized metal species are detected in the dense plasma region of the magnetron, however, up to four-fold ionized Ti metal ions were found.

Figure 3 shows the influence of peak discharge current I_d on plasma composition as derived from Langmuir probe, mass spectroscopy, and atomic absorption spectroscopy. The Ti ion-to-neutral ratio increases with the discharge current. Metal ions are created via direct electron impact ionization during the pulse.

The average ion energy in HIPIMS is typically factor 3 higher than in conventional DC sputtering.

Ion energy distribution functions (IEDFs) of metal ions in HIPIMS consist of two Maxwellian distributions with low and high energy [8]. The low-energy distribution is attributed to fully thermalized metal ions existing in the post-discharge. Whereas the high-energy distribution originates from the sputtering cascade. The high-energy distribution and average ion energy increase with peak discharge current and prevail for materials with high sputter yields [8].
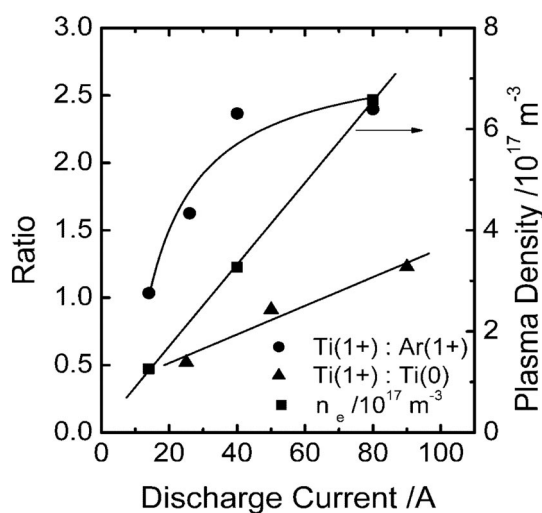
Fig. 3 Metal ion-to-neutral ratio, gas ion-to-metal ion ratio, and plasma density vs. peak target current for HIPIMS of Ti derived from atomic absorption spectroscopy, mass spectroscopy and Langmuir probes, respectively [10].

The main part of gas ions remain at low energy and room temperature. However, due to their interaction with sputtered metal atoms, Ar IEDF exhibits a high energy tail which is significantly lower than that of metal ions.

The HIPIMS current pulse develops through several stages [4]. When voltage is applied, the plasma density in the chamber is negligible and the discharge has to be ignited. An electron wave characterized with high electron temperature of >15 eV propagates through the chamber and initiates ignition [9]. As discharge current starts to flow, it normally exceeds the level for DC within a few microseconds and the discharge dissipates a high power. As a result, the density of gas, especially near the cathode, is reduced [4].

At the same time, as I_d increases, the density of metal neutrals increases after which first single- and later double-charged metal ions are created. At a certain time, the discharge transforms from Ar sputtering to a self-sustained self-sputtering regime [4]. Materials with a higher sputtering yield generate higher plasma density as the number of neutrals and ionization frequency increase.

UP-SCALING

HIPIMS was operated for the first time on large rectangular cathodes with area 440 cm^2 in December 2003 and 1200 cm^2 in January 2004 [11]. The discharge was driven with a power generator HMP 6/16 (Advanced Converters (now Hüttinger Electronic) Sp z o.o., Warsaw, Poland), capable of supplying power pulses with duration in the range 0–200 µs at a frequency of 0–100 Hz (10 ms) equivalent to a duty cycle of 2 %. The power supply was capable of delivering peak currents of up to 3000 A and at a voltage of 2000 V. An arc suppression design allowed switch off of the power supply even at the maximum current. The cathode and power supply were installed in an industrial size batch coater Hauzer HTC 1000/4 (chamber volume of 1 m^3), replacing one of the four original cathodes of the machine. The HIPIMS discharge produced Ti(2+) and Ti(1+) metal ions similar to the plasma compositions found for HIPIMS on laboratory size cathodes with area up to 180 cm^2.

Further up-scaling to cathode area of 1200 cm^2 was carried out on a Hauzer standard cathode. Figure 2 illustrates a great similarity in the *I–U* curves for two cathodes with cathode area of 19 and 1200 cm^2. It is interesting to note that the threshold power density remained the same. Figure 1 displays the maximum voltage and current pulse shapes obtained.

HIPIMS PRETREATMENT

Pretreatment by HIPIMS is carried out to improve adhesion of coatings to the substrate. Typically, the goal of pretreatment is to sputter-remove carbon and oxide contamination in order to free the surface of nucleation sites other than those provided by the substrate crystal. The substrate is biased to a few hundred volts in a plasma environment to carry out sputtering. At energies above 500 V, ions are implanted. Inert ions form no bonds with the surrounding atoms, thus defecting the crystal structure and causing lattice deformation and leading to embrittlement of the substrate as it is brought closer to its yield stress.

In contrast, metal ions such as Cr, Nb, etc. form strong bonds with the atoms of the substrate lattice. The crystallinity of the interface is preserved since implanted metals have high solubility in the host lattice and contribute little strain.

The atomic concentration of elements as a function of distance from the interface was obtained by scanning transmission electron microscopy/energy-dispersive spectrometry (STEM/EDS) analysis for a system comprising: stainless steel 304 substrate, HIPIMS of Nb pretreatment, and CrN deposition. Nb is incorporated at the very interface in a region with width of ~5 nm. The concentration of Ar was very low at ~1 at. %. The ion range and content of Nb can be explained by the magnitude and chemistry of the ion flux. At a bombarding voltage of $U_{BIAS} = -1000$ V, two phenomena occur: substrate resputtering and ion implantation. The substrate resputtering rate is significant because the sputter yield at 1000 eV is high, and at the same time the ion bombardment flux of 300 mA cm^{-2} peak is substantial. Due to the high concentration of metal ions of 65 % in the bombarding flux, the implantation rate exceeds the resputtering rate.

V and CrAlY implantation have also been realized. In particular, the incorporation of yttrium in the interface [12] has been shown to improve oxidation resistance of the subsequent coated system.

Local epitaxy and coating-substrate adhesion

The microstructure of large lengths of the substrate-coating interface was examined [13]. Selected-area diffraction patterns (SADPs) (insets of Fig. 4) of the film and substrate showed parallel alignment, proving unambiguously the cube-on-cube epitaxial orientation between the substrate and coating. This is particularly interesting given the large lattice mismatch of 15 %. The alignment was retained over several microns in lateral direction. Furthermore, the orientation of the coating was found to switch at substrate grain boundaries to follow the orientation of the substrate.

Figure 4 shows a lattice image of an interface prepared by HIPIMS of Cr with $U_{BIAS} = -600$ V. Atomic columns are resolved in both the coating and the substrate, indicating atomic registry between the two lattices. The crystalline structure is preserved throughout the interface region. The atomic planes of the coating are seen to be in direct contact with the atomic planes of the SS substrates throughout the imaged area, thus signifying a fully dense interface. This level of contact can be compared to a grain boundary in bulk materials. No gas bubble formation was present.

The apparent coherency of the coating lattice to that of the substrate results from the intimate bonding between the nitride coating and the substrate. As the nitride layer nucleates, the clean surface promotes direct bonding of the adatoms to the substrate with individual nuclei highly aligned over individual substrate grains due to crystallographic templating. During coalescence, the film nuclei merge without forming grain boundaries. Thus, the grain size of the coating closely duplicates the structure of the substrate, which typically is on the order of micrometres. This mode of interface formation is markedly different from cases when the coating nucleates on substrate grains covered with a layer that is fine grained because of contamination or excessive ion damage. In addition to forming weaker bonding across the interface, the coating nuclei are randomly oriented and form a column size in the nanometre range [13].

Crystallographic templating was observed for several coating-substrate combinations, e.g., $Ti_{0.5}Al_{0.5}N$ base layer on stainless steel with pretreatment by HIPIMS of V as well as for a CrAlN layer grown on a γ-TiAl substrate after HIPIMS of Cr pretreatment.

The large-scale epitaxy discussed in the previous section translates into strong adhesion of the overall coating as measured with scratch testing. Figure 5 presents a comparison between scratch test critical loads L_C for identical CrN/NbN nanolayered coatings where the interface was pretreated by Ar glow discharge, Cr arc, and HIPIMS of Cr. The L_C values for HIPIMS pretreatment are higher than those for arc pretreatment.

The difference may be attributed in part to the more disturbed nature of arc interfaces. The Ar pretreatment resulted in a low adhesion due to insufficient cleanliness of the interface and embrittlement caused by Ar incorporation.
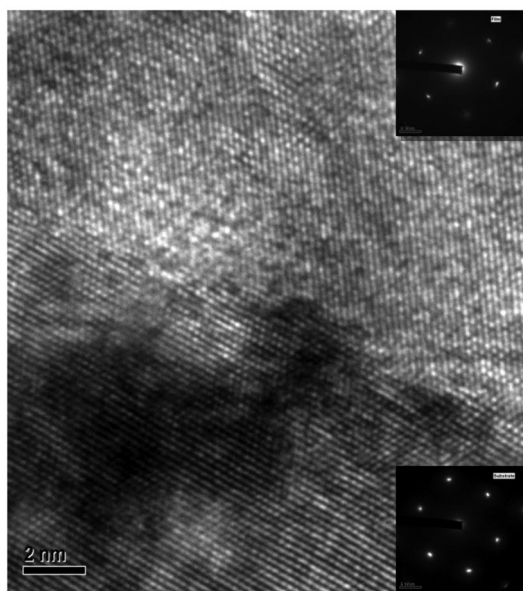
Fig. 4 Cross-sectional lattice imaging of the interface between substrate (bottom) and CrN coating (top) as prepared by HIPIMS of Cr pretreatment, $U_{BIAS} = -600$ V. Insets show diffraction patterns from the film and substrate [13].
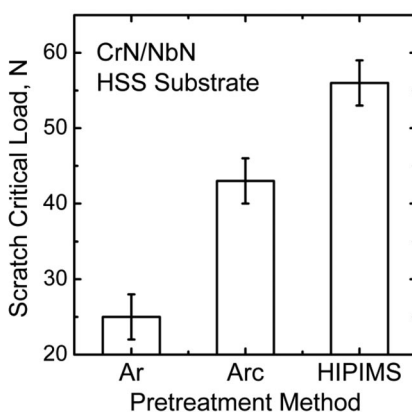
Fig. 5 Adhesion of CrN/NbN coatings on HSS substrate pretreated by Ar glow discharge, cathodic arc, and HIPIMS discharges [13].

Coating performance and applications

The pretreatment alone can have a strong impact on the wear, corrosion, and oxidation performance of the coatings in tests.

Two coating systems have been studied for wear applications. In the CrN system, HIPIMS was used for pretreatment and the coating was deposited by conventional DC magnetron sputtering. The adhesion on high-speed steel (HSS) substrates was >60 N. The friction coefficients were typical for CrN in the range of 0.5. However, sliding-wear rates decreased by a factor of 10 compared to UBM CrN (Fig. 6).
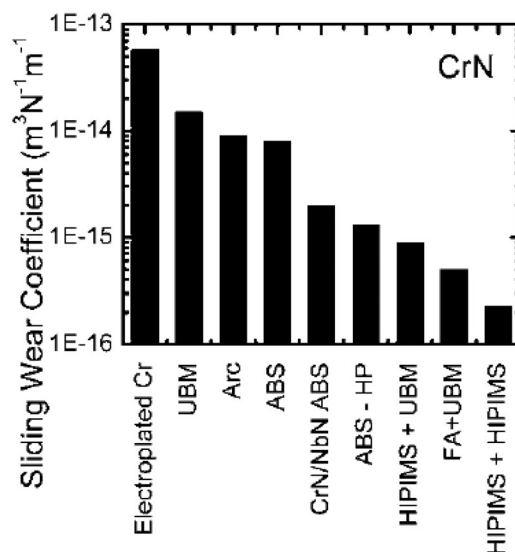
Fig. 6 Sliding-wear coefficients of Cr-based hard coatings [14].

The wear track was very smooth. A strong factor improving the performance in wear is the good adhesion of the coating.

A coating system was developed for difficult-to-machine alloys such as Ti and Al based on a nanolayer coating comprising TiAlCN and VCN layers [15]. Interestingly, the layering in this system was due to the spontaneous vertical segregation of carbon that formed a quasi-periodic structure with a wavelength of 2.8 nm. The friction coefficient was in the range of 0.12 compared to 0.4 for the C-free version (TiAlN/VN) of the same coating. Furthermore, there was no build-up of a tribolayer due to the easier sliding between layers and low roughness of the coating. Thus, although the chemical composition of the coating has a strong influence on the performance, the adhesion and smoothness of the coating achieved by HIPIMS pretreatment were important prerequisites for excellent wear resistance.

In tests of turning Ti, the lifetime of inserts was improved by a factor of 3 compared to uncoated tools. The coating also outperformed DLC coatings by increasing the volume of removed material by a factor of 4 in milling of Si-containing Al alloys for automotive and aerospace applications [15].

Coatings based on Nb are of high interest in corrosion-resistant applications due to their strong passivation behavior. The addition of CrN to NbN improves the wear performance of the coating especially when combined in a nanoscale multilayer stack with a bilayer thickness of 3.5 nm. With the development of HIPIMS, one of the first coating systems to use the HIPIMS pretreatment was the CrN/NbN. HIPIMS-pretreated specimen with Nb interlayer showed excellent passivation behavior with current density of 1×10^{-6} A cm^{-2} at the maximum measured potential of +1000 mV. For cathodic arc

pretreated samples, pitting occurred as the corrosion potential was exceeded and no passivation took place.

Commercial electroplated hard Cr layers were found to provide passivation at potentials up to +880 mV, however, the maximum corrosion current densities and activity were up to three orders of magnitude higher than for the HIPIMS. Thus, the HIPIMS pretreated coating showed a significantly better performance due to the elimination of growth defects.

High-temperature oxidation resistance is a demanding requirement for aerospace engines and energy generation turbines. Improving efficiency requires the replacement of conventional alloys [12] with lighter materials such as γ-TiAl. To extend the operating temperatures above 650 °C, a number of manufacturers have chosen the route of protecting the bulk material with an oxidation- and abrasion-resistant coating. One such coating is the nanolayer system CrAlYN/CrN [12] whose main constituents Cr and Al form dense oxidation-suppressing oxides. Adding nitrogen and nanolayering of the system increases the abrasive resistance. The role of Y is to block grain boundary porosity and inhibits further oxidation. One of the improvements enabled by HIPIMS of CrAlY is the introduction of Y at the substrate-coating interface [12]. Cr, Al, and Y ions are generated in the HIPIMS plasma at the cathode, which are then embedded in the substrate [13].

Densification of the coating has a significant impact on the performance in oxidation due to blocking of inter-columnar diffusion of oxygen. Additionally, the nitride phase of Cr and Al means that they are more stable against corrosion attack. The results from 1000 h exposure in molten salt and corrosive environment with H_2S/H_2O at 1000 °C are given in Fig. 7. Intermetallic coatings AlAu and PtAl exhibit a very high weight gain due to intensive corrosion and oxidation, even more so than the bare γ-TiAl substrate itself. In contrast, the CrAlYN/CrN nanolayer coating is able to protect the substrate and inhibits the hot corrosion process by reducing the weight gain by a factor of 2.
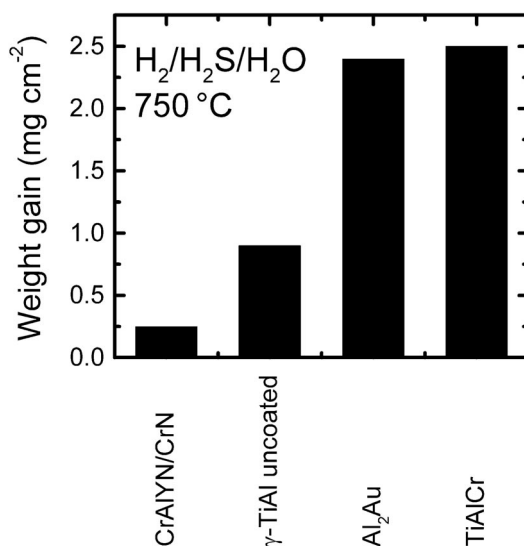
Fig. 7 Weight gain after 1000 h exposure to $H_2/H_2S/H_2O$ at 750 °C of HIPIMS-pretreated CrAlYN/CrN [12].

COATING BY HIPIMS

Undoubtedly, one of the strong advantages of HIPIMS is its use as a deposition process. The high degree of ionization of the deposition flux brings advantages in densifying the structure and improving performance in a wide range of applications of thin film and coatings. The development of the deposi-

tion process has evolved from the first metal layer and simple nitride deposition to oxide and nanolayer deposition.

One of the first depositions by HIPIMS in inert gas (Ar) atmosphere was demonstrated for Cu by Kouznetsov et al. [3], who estimated an ionization degree of the deposition flux of 70 %. Cu films were then deposited by HIPIMS and successfully filled trenches with aspect ratio of 1:1. Later, Ti and Ta deposition were demonstrated with improved crystallinity and high ionization.

Single nitride CrN films were deposited by a two-step process where HSS substrates were pre-treated in HIPIMS of Cr plasma and the coating was then deposited by HIPIMS of Cr in a mixed Ar and N_2 atmosphere. During the deposition process, the nitrogen was highly activated with atomic ions and strong presence of a molecular ion N_2^+ peak. Only the CrN phase was detected at Ar:N_2 partial pressure ratios from 1:1 to 1:5. Transmission electron microscopy (TEM) showed a fully dense microstructure.

Repeated nucleation was observed and columnar boundaries were obscured due to intensive exchange of adatoms between columns. The growth could be described as a mixture of the transition phase and equiaxed structure as defined in the Thornton zone model. The column tops were flat. The adhesion of the 2 μm coating was excellent with scratch test critical load value of $L_C > 85$ N on HSS.
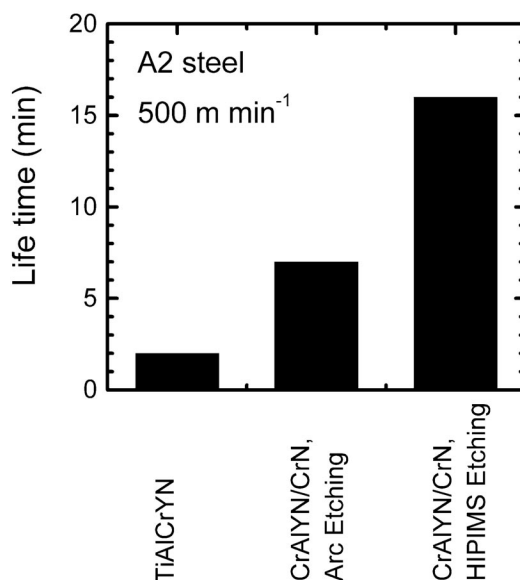
Fig. 8 Lifetime of tools coated by CrAlYN/CrN when milling A2 steel.

HIPIMS-deposited CrN were the best performers in comparative potentiodynamic corrosion tests with electroplated hard Cr and arc-deposited CrN with corrosion currents and activity reduced by a factor of 10–100. The better performance is attributed to the fully dense droplet-free microstructure.

In sliding-wear pin-on-disk tests, the HIPIMS-deposited coating exhibited a friction coefficient of 0.45 against Al_2O_3 and was maintained over a sliding distance of 23 km. The wear track was smooth, indicating a stable, low-wear process. The wear coefficient was low at 2.2×10^{-16} mNm^{-3}.

Improvements are also seen in abrasive wear resistance and impact fatigue resistance due to the high density of the microstructure.

A wide range of oxide coatings have been grown by HIPIMS. Due to the high plasma density of the process, it is expected to have a wider operating window than conventional DC magnetron sputter-

ing. Similar conditions as HIPIMS are present in the arc discharge, which is known to have low poisoning hysteresis.

InSnO (ITO) is applied in flat panel displays due to its high transparency and low electrical resistivity. The coating is typically deposited by magnetron sputtering to ensure that the deposition vapor contains no macroparticles and to avoid any defects in the display panel itself. A high ion-to-neutral ratio is key to obtaining a smooth surface and high transparency. In a typical magnetron sputtering in-line coater, masking is used to ensure only areas with high ion bombardment are coated.

The best coatings deposited by masked DC sputtering exhibited a resistivity of $\rho = 5000$ μΩcm and visual absorption was still maintained at $\alpha_v = 2$ %. In comparison, HIPIMS deposition was carried out without masking [16]. Here, the best resistivity of $\rho = 3100$ μΩcm was considerably lower and the visual absorption of $\alpha_v = 4$ % was comparable to the DC case. The improved resistivity and visual absorption of HIPIMS coatings is due to the high ionization of the HIPIMS discharge.

Because masking was avoided during HIPIMS deposition, the net deposition rate was considerably greater than DC. The low deposition temperatures and high rates of the HIPIMS process make it a viable alternative to DC and MF.

Titanium dioxide (TiO_2) films have been deposited utilizing HIPIMS by several authors [17]. Consistently, the deposition rate for this material is reported higher than the DC case. The desired rutile phase formed readily on conducting substrates [17]. Coatings deposited by HIPIMS exhibited higher refractive index, signifying a low roughness of the coating due to the high ionization of the technology. The crystallinity was also improved.

Zinc oxide (ZnO) is used as a seed layer for low-emissivity, silver-based, multilayered stacks employed in low-emissivity windows where it is crucial to produce a smooth surface and ensure sharp interfaces with silver layers. ZnO films deposited by HIPIMS were found to be smoother and showed a lower peak-to-valley rugosity compared to DC [18]. The deposition rate for HIPIMS and DC bipolar magnetron sputtering were similar.

Because of metal ion or background gas bombardment and metal ion condensation, the growth mechanism is different for HIPIMS. Ion irradiation and condensation induced the formation of more nucleation clusters because of enhanced surface diffusion, while also preventing the growth of thick columns with voids because of resputtering and redeposition. This makes the film denser with smaller nodules and a smoother surface.

CrN/NbN nanoscale multilayer coatings were deposited with a bilayer thickness of 3.5 nm by the combined HIPIMS and unbalanced magnetron (UBM) sputtering technology [19]. During the HIPIMS stage of the deposition, the coatings grow under conditions of highly energetic ion bombardment where metal ions and highly reactive dissociated N+ ions comprise the main fraction of the flux, thus contributing to densification of the films with their high mobility. In the UBM stage of deposition, the flux comprises mainly gas ions that contribute their energy indirectly in the case of Ar and deliver half the energy upon dissociation of N_2.

The surface of the HIPIMS films was considerably flatter with somewhat smaller column size as compared to the dome-shaped broad columns in the UBM. In the HIPIMS case, the structure was fully dense (Fig. 9a) and some column boundaries are obscured, indicating a strong intercolumnar connection and high intercolumnar density. In contrast, in the UBM case the columnar boundaries were strongly defined by the presence of voids (Fig. 9b).

The sliding-wear friction coefficient was 0.2 for the smooth HIPIMS coatings compared to 0.45 for the UBM. The wear coefficient was reduced by a factor of 4 in the case of HIPIMS. This can be attributed to the strong contact between columns that provide support to each other during sliding wear.

In corrosion, the HIPIMS coating (Ecorr = + 400 mV) was more noble as compared to UBM coatings (Ecorr = + 332 mV). HIPIMS coatings had up to 100 times lower corrosion current densities compared to UBM.
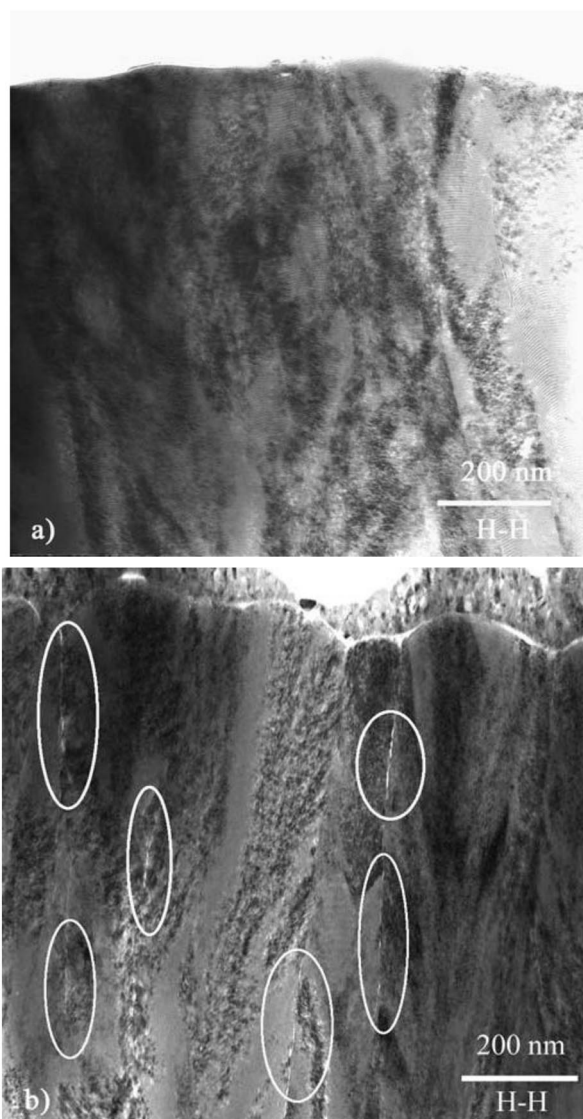
Fig. 9 TEM micrographs showing microstructure details: (a) defect-free H–H coating (b) H–U coating evident with intercolumnar voids (marked with circles) [19].

CONCLUSIONS

In summary, HIPIMS is a high-current quasi-stationary glow discharge that produces high plasma densities and metal deposition flux with significant degree of ionization. Doubly and triply charged metal ions are observed. The technology has been up-scaled successfully to industrial production equipment. HIPIMS can be used for pretreatment to enhance adhesion by promoting epitaxial growth of nitride coatings on steel, carbide, and intermetallic substrates. HIPIMS has been successfully utilized to deposit coatings with high-density microstructure and excellent performance in wear, corrosion, and oxidation, but also optical applications.

ACKNOWLEDGMENTS

REFERENCES

1. O. A. Malkin. *Impulsnij tok i Relaksatsija w Gaze*, Atomizdat, Moscow (1974).
2. P. M. Tyuryukanov, I. K. Fetisov, G. V. Khodachenko. *Soviet Phys., Tech. Phys.* (Engl. trans. of *Z. Tekh. Fiz.*) **23**, 923 (1978).
3. V. Kouznetsov, K. Macak, M. Schneider, J. U. Helmersson, I. Petrov. *Surf. Coat. Technol.* **122**, 290 (1999).
4. A. P. Ehiasarian, R. New, W. D. Munz, L. Hultman, U. Helmersson, V. Kouznetsov. *Vacuum* **65**, 147 (2002).
5. J. Bohlmark, M. Lattemann, J. T. Gudmundsson, A. P. Ehiasarian, Y. Aranda Gonzalvo, N. Brenning, U. Helmersson. *Thin Solid Films* **515**, 1522 (2006).
6. J. T. Gudmundsson, J. Alami, U. Helmersson. *Appl. Phys. Lett.* **78**, 3427 (2001).
7. J. Vlcek, P. Kudlacek, K. Burcalova, J. Musil. *J. Vac. Sci. Technol. A* **25**, 42 (2007).
8. A. Hecimovic, K. Burcalova, A. P. Ehiasarian. *J. Phys. D: Appl. Phys.* **41**, 095203 (2008).
9. A. Vetushka, A. P. Ehiasarian. *J. Phys. D: Appl. Phys.* **41**, 015204 (2008).
10. A. P. Ehiasarian, A. Vetushka, A. Hecimovic, S. Konstantinidis. *J. Appl. Phys.* 104 (2008).
11. A. P. Ehiasarian, R. Bugyi. In 47th Annual Technical Conference Proceedings, April 2004, pp. 437–441, Society of Vacuum Coaters, San Francisco (2004).
12. P. E. Hovsepian, C. Reinhard, A. P. Ehiasarian. *Surf. Coat. Technol.* **201**, 4105 (2006).
13. A. P. Ehiasarian, J. G. Wen, I. Petrov. *J. Appl. Phys.* **101**, 54301 (2007).
14. A. P. Ehiasarian, P. E. Hovsepian, L. Hultman, U. Helmersson. *Thin Solid Films* **457**, 270 (2004).
15. P. E. Hovsepian, A. P. Ehiasarian, A. Deeming, C. Schimpf. *Plasma Process. Polym.* **4**, S897 (2007).
16. V. Sittinger, F. Ruske, C. Gerloff, W. Werner, B. Szyszka, D. J. Christie. In 49th Annual Technical Conference Proceedings, April 2006, pp. 343–348, Society of Vacuum Coaters, Washington, DC (2006).
17. S. Konstantinidis, J. P. Dauchot, M. Hecq. *Thin Solid Films* **515**, 1182 (2006).
18. S. Konstantinidis, A. Hemberg, J. P. Dauchot, M. Hecq. *J. Vac. Sci. Technol. B* **25**, L19 (2007).
19. Y. P. Purandare, A. P. Ehiasarian, P. E. Hovsepian. *J. Vac. Sci. Technol. A* **26**, 288 (2008).